

# Water Conservation & Management (WCM)

DOI: http://doi.org/10.26480/wcm.03.2025.481.489



ISSN: 2523-5672 (Online) CODEN: WCMABD

RESEARCH ARTICLE

# MODEL-BASED ESTIMATION OF COASTAL MORPHODYNAMIC CHANGES CAUSED BY SEA TOLL ROAD DEVELOPMENT IN THE NORTHERN COAST OF JAVA, INDONESIA: ITS IMPLICATIONS FOR SEDIMENT DYNAMICS

Indra Hermawana\*, Sutrisno Anggoroa, Suradi Wijaya Saputraa, Agus Suhermanb, Wisnu Arya Gemilangc, Ulung Jantama Wishad

- <sup>a</sup>Department of Aquatic Resources Management, Faculty of Fisheries and Marine Science, Diponegoro University, Semarang 50275, Indonesia
- Department of Capture Fisheries, Faculty of Fisheries and Marine Science, Diponegoro University, Semarang 50275, Indonesia
- Center for Marine and Fisheries Training, Ministry of Marine Affairs and Fisheries, Central Jakarta, Jakarta 10110, Indonesia
- <sup>a</sup>Research Center for Oceanography, National Research and Innovation Agency (BRIN), North Jakarta, Jakarta 14430, Indonesia
- $\hbox{\it *Corresponding Author Email: indrakemenko@gmail.com}\\$

This is an open access journal distributed under the Creative Commons Attribution License CC BY 4.0, which permits unrestricted use, distribution, and reproduction in any medium, provided the original work is properly cited

#### **ABSTRACT**

#### Article History:

Received 11 April 2025 Revised 21 May 2025 Accepted 17 June 2025 Available online 25 July 2025 The Semarang-Demak coastline of northern Java, Indonesia, faces severe erosion and land subsidence driven by tidal forcing, sediment transport, and human interventions. This study evaluates the impacts of the Semarang-Demak Sea toll road on hydrodynamics, sediment dynamics, and seabed morphology. Field data were collected through sediment sampling, tidal and current measurements, and monitoring of suspended sediments. A coupled hydrodynamic-sediment transport model (MIKE 21/3) was developed to simulate tidal currents, sediment dispersion, and bed level change. Results indicate a mixed, predominantly diurnal tidal regime, dominated by O1 and K1 constituents. Current simulations have revealed significant spatial variability, with spring ebb tides generating seaward flows exceeding 0.6 m/s, which enhance sediment resuspension and export, while neap tides promote fine sediment deposition. Suspended sediment concentrations were notably higher during spring tides, particularly in mid-reach zones of convergent flow. Bed level change modeling identified critical erosion near Tanjung Emas Port and Bedono, as well as depositional zones offshore of Sriwulan and Demak. Importantly, the toll road corridor intersects dynamic sediment redistribution areas, posing risks of localized scour, differential settlement, and altered flow pathways that could compromise structural stability and increase coastal hazards. These findings underscore the importance of integrated sediment management, continuous monitoring, and adaptive engineering approaches in mitigating infrastructure impacts and fostering long-term coastal resilience.

### KEYWORDS

Hydrodynamics, sediment transport, coastal erosion, Semarang-Demak, bed level change.

#### 1. Introduction

From a geochronological perspective, the northern coast of Java, Indonesia, is predominantly composed of unstable soils, primarily swamp deposits, which increase the region's susceptibility to erosion and coastline change (Solihuddin et al., 2024). This vulnerability has been further exacerbated by extensive mangrove degradation resulting from rapid urban development over the past few decades, which intensifies the threats to coastal stability (Gemilang et al., 2020). For example, the Semarang-Demak coastline has experienced severe coastal degradation, including coastline retreat, erosion, and tidal flooding, which continue to affect several coastal villages such as Bedono, Timbulsoko, and Sriwulan (Ismanto et al., 2017). As reported that an estimated 495.8 hectares of coastal land had been eroded, leading to the loss of mangrove forests and coastal settlements, the destruction of aquaculture ponds, the decline of coastal resources and ecosystems, and the emergence of socio-economic challenges (Marfai et al., 2016).

In addition to coastal issues, excessive groundwater extraction is widely regarded as a major factor contributing to significant land subsidence along the Semarang–Demak coast (Andreas et al., 2018). This subsidence

has exacerbated flood inundation, submerging more than 16 coastal villages and extensive settlement areas (Astusti et al., 2018). The combined effects of sea level rise, land subsidence, and coastal degradation, driven by land-use changes, are considered the primary drivers of coastal damage in the Semarang–Demak region (Rimba et al., 2018; Chrysanti et al., 2024). Furthermore, the conversion of mangrove forests into aquaculture ponds, which began in the 1980s, has heightened the region's coastal vulnerability (Van Wesenbeeck et al., 2015). This large-scale land conversion was accompanied by the construction of breakwaters around the ponds, altering the coastal hydrodynamics (Gemilang et al., 2020). The resulting changes in sediment transport, compounded by the alluvial nature of the Semarang–Demak coastline, have led to severe erosion and flooding, which are practically unavoidable under current conditions (Chrysanti et al., 2024).

In order to address the issue of coastal erosion, the central and local governments, along with various stakeholders, initiated the implementation of Hybrid Engineering (HE) in 2013 (Sugianto et al., 2022). HE is a nature-inspired, permeable coastal structure that utilizes locally available and environmentally friendly materials to promote coastal restoration by enhancing natural sedimentation in eroded areas (Hafid et al., 2021). This approach proved effective in increasing the sedimentation

Quick Response Code

Access this article online



Website: www.watconman.org DOI:

10.26480/wcm.03.2025.481.489

rate in Sayung Subdistrict, particularly in Timbulsloko Village, where an average rate of 0.41 cm/year was recorded between 2013 and 2015, accompanied by a significant expansion of mangrove cover, with approximately 46 hectares restored during the same period (Gemilang et al., 2020). However, despite the successes of HE in specific locations, unprotected areas continued to erode, creating new challenges for coastal stability (Baskoro et al., 2016). Over time, the temporary nature of the HE structures limited their effectiveness in halting coastline retreats, ultimately leading to intensified coastal hazards and flooding risks.

In recent years, the Indonesian government has invested significant effort and resources in improving the main road infrastructure along the northern coast of Java, aiming to enhance mobility and distribution (Pamungkas, 2021). The Semarang-Demak coastal corridor, in particular, serves as a critical transportation route linking Semarang City and Demak Regency. According to the Ministerial Decree of Public Works and Housing No. 355/KPTS/M/2017 on the integration and development of the Semarang Sea Embankment and Semarang-Demak Toll Road, the alignment of the existing main road is being redirected to the newly developed sea toll road, which is integrated with the sea embankments. Despite the challenges posed by a complex land acquisition process, this coastal zone has already suffered from significant degradation, high hazard risks, and widespread flooding, necessitating land reclamation efforts (Dewi and Bijker, 2020). Persistent flooding has led to a decline in land value (Ismail et al., 2016). However, this development has also created dilemmas, disrupting public services, affecting socioeconomic activities, and resulting in the loss of productive land (Shrestha et al., 2019).

Recent reports indicate that increased seawater inundation and flooding have further impacted the Semarang-Demak main road, elevating the issue to a national concern. These impacts are primarily attributed to hydrodynamic alterations caused by the construction of the sea toll road (Jamaludin and Mahdi, 2025). The filling of previously inundated coastal zones has disrupted local hydrodynamic regimes, altered sediment transport processes, and exacerbated coastal erosion (Jafarzadegan et al., 2023). These challenges highlight the need for an integrated study to assess the hydrodynamic shifts and morphological changes that occur following the development of the sea embankment and toll road. A hydrodynamic modeling approach offers a promising method for estimating environmental changes, particularly when combined with realtime measurements to validate the model and predict the potential impacts on the degraded coastal zone (Wisha et al., 2022). Hydrodynamic models have been widely applied to analyze changes in water movement, sediment transport, morphological evolution, and environmental or ecological conditions (Hamidifar et al., 2024; Wisha et al., 2018; Yuan et al., 2021).

In this study, we assess the sediment distribution patterns, changes in hydrodynamic regimes, and sediment transport-induced morphological alterations following the construction of the Semarang–Demak Sea toll road. Additionally, we project future coastal conditions through modeling simulations that incorporate sea level rise scenarios. Our central hypothesis is that significant changes in tidal current patterns, driven by the development, will intensify erosion near the sea embankment and the toll road, increasing coastal vulnerability and flood risk. Therefore, this study aims to evaluate the impacts of the sea toll road on coastal stability and morphology, as well as to provide future projections under the assumption that no advanced mitigation measures are implemented to address these pressing coastal issues.

# 2. MATERIALS AND METHODS

#### 2.1 Study site and field observation

The north coast of Java is geologically composed of young volcanic deposits, alluvial sediments, and coastal deposits, which are generally loose and unconsolidated materials (Solihuddin et al., 2021). The Quaternary sediments in this region primarily consist of tuffaceous claystone, sand, silt, and clay. Specifically, the primary sediment type along the Sayung Coast in Demak is alluvial deposits (Qa), which include gravel, sand, clay, and silt. The Demak area is also bordered by volcanic rocks, such as the Muria Tuff (Qvtm) and Muria Lava (Qvlm) in the northeastern part. In contrast, the eastern part is bordered by the Bulu Formation (Tmb), which consists of interbedded limestone, sandy limestone, and clay limestone (Gemilang et al., 2020).

The Semarang-Demak region is tectonically influenced by strike-slip fault systems, as evidenced by several lineaments observed on the Kudus and Magelang-Semarang regional geological map. Additionally, the subsurface geological structure of Demak, characterized by weak zones prone to movement, contributes to land subsidence, which in turn exacerbates

surface tidal flooding (Sarah et al., 2020). Moreover, the presence of the Muria–Kebumen and Pamanukan–Cilacap standard fault systems further complicates Central Java's tectonic setting. These two significant strike-slip faults have caused the northern part of Central Java to subside. In contrast, the southern part has been uplifted, creating a distinct geological contrast across the region (Satyana, 2006).

The Semarang–Demak Toll Road Project, a National Strategic Project in Central Java, aims to enhance regional connectivity, particularly by linking industrial areas and ports in Demak. Spanning 27 km, the toll road is designed to reduce travel times and ease traffic congestion. Additionally, it functions as a key component of a flood control system by integrating a sea embankment, polder system, and drainage infrastructure to manage tidal flooding (Pamungkas, 2021).

Construction began in late 2019, with the 16 km section temporarily opened for use during holiday seasons to ease congestion, followed by further improvements and inspections. However, the project raises environmental concerns, as it will clear approximately 46 hectares of mangrove forests in Semarang and Demak, potentially exacerbating coastal vulnerability in the region (Solahudin et al., 2024). In addition to the hydrodynamic change, the construction is likely to have altered the tidal current pattern-driven sediment movement mechanism, thereby increasing the risk of coastal hazards in the locality.



Figure 1: Location of the Semarang-Demak Sea toll road development

Bottom sediment sampling was carried out on 3–4 March 2020 at ten sampling points distributed across the Semarang–Demak Sea toll road construction site (Figure 1). The sampling locations were selected based on coastal morphological characteristics, including tidal flats, offshore areas, estuarine zones, and protected regions such as mangrove forests and Hybrid Engineering (HE) sites. Sampling was conducted at water depths ranging from 1.5 to 3.5 meters using an Ekman grab sampler (Model 196-B15).

The collected sediment samples were analyzed in the laboratory to determine grain size distribution using the granulometric analysis method (Hubbard and Pocock, 1972, Hsieh, 1995). Grain sizes were classified through a series of sieves with mesh sizes of >2 mm, 1.4 mm, 1 mm, 0.5 mm, 0.250 mm, 0.150 mm, 0.090 mm, 0.063 mm, and <0.063 mm. This analysis helps assess the resistance of sediment grains to exogenic processes such as weathering, erosion, abrasion, and sediment transport and deposition (Yasin et al., 2016). Grain size classification followed the Wentworth scale, while sediment types were identified using the Shepard ternary diagram (Dyer, 1986; Wentworth, 1922). Additionally, sediment statistical parameters, including sorting, skewness, and kurtosis, were calculated to interpret sediment distribution patterns, transport mechanisms, and depositional processes based on (Folk and Ward, 1957). To determine the hydrodynamic profile of the study area and validate the modeling results, in-situ tide measurements were conducted using a Valeport tide gauge over 30 days (from January 31 to March 8, 2020), positioned near the sea toll road construction site (Figure 1). The instrument recorded water levels at 30-minute intervals with an accuracy of ±10 mm. Additionally, two Valeport current meters were deployed simultaneously for approximately 24 hours during both spring and neap tide conditions (3-10 March 2020) in the offshore zone, specifically in the north (A1) and west (A2) parts of the toll road construction area (Figure 1). These measurements captured current velocities at the surface, with 5minute intervals to assess the current-driven sediment transport in the study area.

#### 2.2 Hydrodynamic and sediment transport model simulation

A coupled flow model hydrodynamic simulation, performed using the MIKE 21/3 modeling package, was employed to assess hydrodynamic conditions in the study area, specifically after the construction of the sea

toll road. This flow modeling approach encompassed simulations of hydrodynamic (HD), spectral wave (SW), mud transport (MT), and sand transport (ST) modules simultaneously. The model domain was constructed using a flexible mesh with element areas ranging from 13 to 21,980  $\,\mathrm{m}^2$ , a maximum of 100,000 nodes, and a minimum allowable angle of 26° (Figure 2).

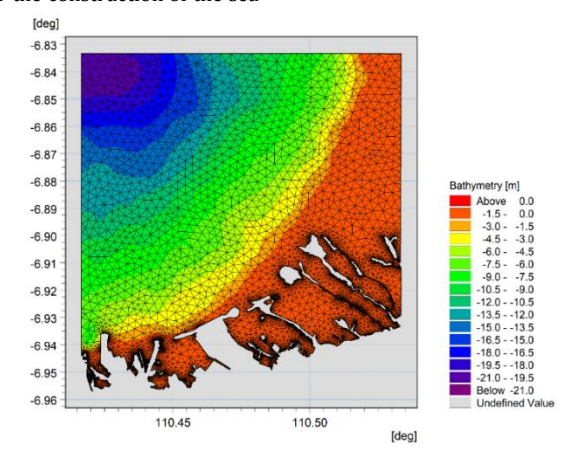


Figure 2: Bathymetry profile and model domain used in this study

Two primary open boundaries were chosen, representing the influence of ocean currents from the north (BC1) and west (BC2). Surface elevation data were utilized across these boundaries and were maintained throughout the simulation. In this case, we initially simulated tidal model programs, such as NAO99b and ERG programs, to estimate surface elevation data. On the other hand, we also considered wind-forcing potential within the simulation as the primary driver of ocean wave generation in the study area. Therefore, we utilized monthly wind data at a height of 10 meters, retrieved from the ERA5 dataset, which consists of u- and v-velocity components with a horizontal resolution of 0.25 degrees.

After validating the HD and SW modeling results, two additional simulations, MT and ST, were run to estimate various sedimentary processes, including erosion, transport, settling, and deposition of cohesive and non-cohesive sediments. At this stage, we also considered the field-measured sediment characteristics that had been previously analyzed. These sediment modeling simulations yield information on sediment transport mechanisms, suspended sediment concentrations, bed level changes, and other morphological features in the study area. The overall modeling setup is presented in Table 1.

Table 1: The input parameters of the model simulation				
Parameters	Applied in the simulation			
HD module				
Seawater density $(kg/m^3)$	1026			
Time step (s)	600			
Manning number $(m^{1/3}/s)$	0.026 - 0.058			
Flood and Dry	Drying depth = 0.01 m Flooding depth = 0.05 m Wetting depth = 0.1 m			
Eddy viscosity	Smangorinsky formulation = $0.28$ Eddy parameters = $1.8e^{-0.006} - 10^7 \frac{m^2}{s^2}$			
SW module				
Water level condition	Reiterated from HD modules			
Wind forcing	Time series of ERA5 wind data (speed and direction)			
Energy transfer	Include quadruplet-wave interaction Include triad-wave interaction-transfer coefficient of 0.25			
Boundary condition	Wave parameters: Significant wave height, Hm0 0.4 m Peak wave period, Tp 8 sec. Mean wave direction, MWD 45° Directional spreading index, n=5			
MT and ST modules				
Water column parameters	Settling velocity coefficient = $0.25 m/s$ Critical shear stress = $0.07 N/m^2$			
Bed parameters	Erosion coefficient = $5 \times 10^{-5} \text{ kg/m}^2/\text{s}$ Critical shear stress = $0.2 \text{ N/m}^2$ Power of erosion = $1$ Density of bed layer = $400 \text{ kg/m}^3$			

	Bed roughness = 0.001 m		
Table 1(Cont.): The input parameters of the model simulation			
Forcing	Reiterated from HD and SW modules		
	Fraction concentration = 0 kg/m <sup>3</sup>		
Initial condition	Layer thickness = 1 m		
	Fraction distribution 100		
Source	Fraction concentration = 0.03 kg/m <sup>3</sup>		

#### 2.3 Model accuracy test

The hydrodynamic-integrated sediment transport modeling results were validated using field-measured data. These data were examined based on several statistical-based approaches, such as correlation coefficients, standard deviation, root mean square errors (RMSE), mean absolute error (MAE), and relative errors. In this case, the assessed dataset included surface elevation, current velocity, and total suspended sediment (TSS) concentrations.

#### 3. RESULTS

#### 3.1 Bottom sediment characteristics

The sediment texture distribution map of the Semarang–Demak coastal region reveals a spatially varied and hydrodynamically dynamic depositional environment along the northern Java Sea. Based on granulometric analysis of ten sediment samples collected in the vicinity of the Semarang–Demak Sea Toll Road development, four primary sediment types were identified: sand, sandy silt, silty sand, and silt. The spatial distribution of these sediments, as illustrated in Figure 3 and Table 3, indicates a distinct zonation pattern. Coarser sediments, particularly sand, are predominantly located near the toll road construction corridor, suggesting high-energy conditions that favor the transport and deposition of larger grain sizes. In contrast, finer sediments such as silt and clay are more concentrated along the nearshore coastline and in the offshore zone, where lower-energy conditions allow finer particles to settle.

This spatial trend is supported by broader granulometric trends analyzed using the Shepard ternary diagram, which classifies silt as the dominant grain size throughout much of the study area. Texture classifications derived from this analysis include sand, silty sand, silt, and clayey sand, with sand and sandy silt emerging as the most frequently observed textures. These results align closely with the sediment distribution map, which shows sandy silt and clayey sand dominating the central zone off Bedono, an area likely shaped by strong tidal forcing and river discharge convergence. The offshore areas exhibit finer fractions, such as silt and silty clay, indicating sediment deposition in lower-energy marine conditions.

Closer to shore, especially along coastal segments near Trimulyo, Terboyo Wetan, and Sriwulan, sediments are predominantly composed of clay, silt, and silty clay, reflective of estuarine mudflat environments. These fine-grained textures are indicative of sedimentation under reduced current velocity, consistent with tidally influenced depositional settings. From a coastal management perspective, these zones present the potential for mangrove habitat restoration and conservation, particularly where historical degradation has occurred.

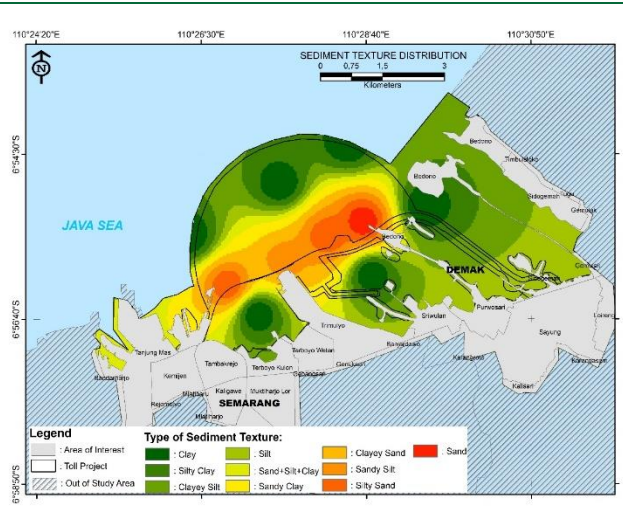


**Figure 3:** Percentage and sediment type distribution in the study area based on Shepard diagram 1954.

Table 3: Summary of dominant sediment type by zone				
Zone	Dominant sediment types	Hydrodynamic Interpretation		
Offshore (North)	Silt, silty clay	Low-energy, fine deposition		
Central Plume (Bedono)	Clayey sand, sandy silt	High-energy, active transport zone		
Coastline (Demak- Semarang)	Silty clay, clay, Deposition zones, suita for restoration			
Toll route intersection	Sandy silt, sandy clay	Potential instability of sediment remobilization		

#### 3.2 Fortnightly tide and sea current features

Table 4 presents the harmonic analysis of tidal constituents based on field observations in the study area. The dominant constituent is the O1 lunar diurnal tide, with an amplitude of 0.56 m, indicating that diurnal tides strongly influence the tidal regime. This condition is further supported by the notable presence of the K1 constituent (0.172 m), another lunar diurnal component. Among the semidiurnal constituents, M2 (0.117 m) and S2 (0.061 m) are present but less prominent, suggesting a mixed tide with diurnal dominance, consistent with a Formzahl value greater than 1.0.

Table 4: Tidal constituent's amplitudes and phases based on the field observations					
Tidal Constituents	Amplitude (m)	Phase (°)	Angular Frequency (Degree/hour)	Species	
M2	0.117	272.72	28.98	Principal lunar semidiurnal	
S2	0.061	192.68	30.00	Principal solar semidiurnal	
K1	0.172	11.25	15.04	Lunar diurnal	
01	0.56	209.74	13.94	Lunar diurnal	
M4	0.003	90.92	57.97	Shallow water overtides of principal lunar	
MS4	0.002	275.47	58.98	Shallow water quarter diurnal	

The inclusion of shallow water constituents such as M4 and MS4, albeit with small amplitudes (0.003 m and 0.002 m, respectively), reflects nonlinear tidal interactions, likely driven by estuarine bathymetry, friction, and shallow depth effects. The angular frequencies correspond well with their expected values, reinforcing the reliability of the harmonic

decomposition. Overall, the tidal characteristics indicate a mixed, mainly diurnal system, typical of many Indonesian estuaries. The dominance of diurnal constituents has significant implications for hydrodynamic behavior, influencing current asymmetry, sediment transport patterns, and tidal inundation cycles. Accurate representation of these constituents

is crucial for reliable tidal modeling and predicting estuarine responses to future environmental changes, such as sea-level rise.

Figure 4 illustrates current rose diagrams for two monitoring stations (CM-01 and CM-02) under different tidal conditions, neap and spring tides, providing insight into the spatial and temporal variability of current direction and speed in the study area. At Station CM-01 during neap tides (Figure 4A), current flow is bidirectional, predominantly oriented northward and southeastward, with secondary flow to the southwest. The current speeds are relatively strong, with a significant proportion of the flow falling within the 0.25–0.35 m/s range and a notable presence of speeds exceeding 0.35 m/s. This result indicates an active hydrodynamic

regime during neap tides, potentially influenced by tidal convergence or topographic effects. In contrast, during spring tides at CM-01 (Figure 4B), the current pattern becomes more unidirectional, with flow concentrated toward the northeast and northwest. However, the current speeds are generally lower, with most values concentrated below 0.15 m/s. This unexpected reduction in current strength during spring tide may reflect localized hydrodynamic damping, such as flow attenuation in a partially enclosed or friction-dominated zone.

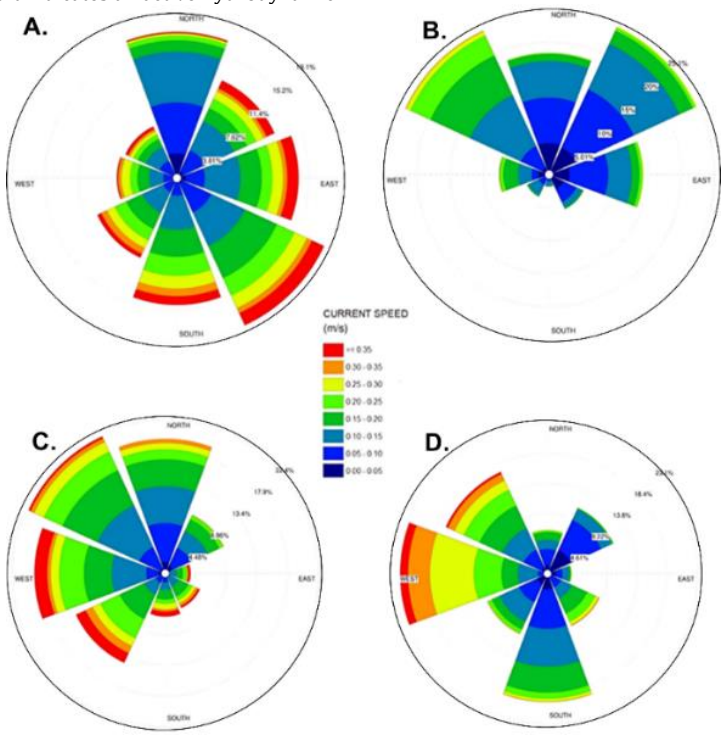
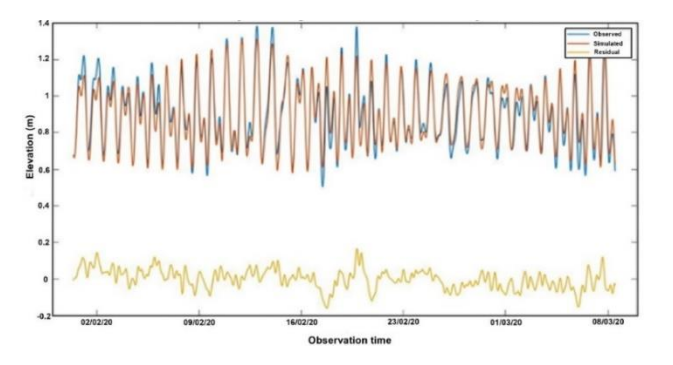


Figure 4: Current rose diagrams of the study area during neap tides (A) and spring tides (B) at station CM-01, and during neap tides (C) and spring tides (D) at station CM-02.

At Station CM-02, the current regime differs considerably. During neap tides (Figure 4C), current flow is broadly distributed but predominantly directed toward the north and west. Speeds range from moderate to high, with frequent values exceeding 0.30 m/s, particularly toward the west. This result suggests that CM-02 is more exposed to open tidal exchange or occupies a channelized flow path. Under spring tide conditions (Figure 4D), the current direction at CM-02 becomes more concentrated toward the west and northwest, with a significant increase in higher current speeds. This station exhibits the strongest currents observed across all conditions, with a substantial portion of flow exceeding 0.30 m/s and even surpassing 0.35 m/s in frequency. These patterns confirm the expected intensification of tidal energy during spring tides and highlight the spatial contrast between CM-01 and CM-02 in terms of flow exposure and tidal response. Overall, the rose diagrams indicate that Station CM-02 experiences stronger and more unidirectional currents, particularly during spring tides, which likely facilitates sediment transport and erosion processes. In contrast, Station CM-01 displays more variable and sometimes weaker flow patterns, suggesting conditions favorable for sediment deposition. These distinctions in current dynamics are critical for understanding local sediment transport regimes and for informing the calibration of hydrodynamic and sediment transport models in the region.



 $\textbf{Figure 5:} \ \textbf{Tidal elevation and analysis data observed in the study area}$ 

Figure 5 displays a time series comparison between observed and simulated tidal elevations over approximately five weeks (from early February to early March 2020). The blue curve represents the observed tidal elevation, the red curve shows the simulated results from the numerical model, and the yellow line represents the residual, i.e., the difference between observed and simulated values. The figure demonstrates a strong agreement between the observed and simulated tidal elevations, with both curves closely overlapping throughout the observation period. This indicates that the numerical model effectively captures the temporal pattern, amplitude, and phase of tidal fluctuations in the study area. The residuals, which mostly range between ±0.05 m and rarely exceed ±0.10 m, are relatively small and show no systematic bias over time. This suggests that the model does not consistently overestimate or underestimate the tidal elevation. The tidal signal exhibits typical mixed semi-diurnal behavior, characterized by a noticeable variation in tidal amplitude over time due to the spring-neap tidal cycle. Peaks and troughs in both observed and simulated data occur at consistent intervals, indicating the model's ability to reproduce tidal dynamics accurately. Overall, the low residual values and the strong visual overlap between the observed and simulated data confirm that the tidal model is well-calibrated for the study area and is reliable for use in subsequent hydrodynamic and sediment transport simulations.

## $3.3\ Tidal\ current\ patterns\ after\ the\ development\ of\ sea\ toll\ road$

Figure 6 illustrates the simulated surface current distribution in the Semarang–Demak coastal area during spring tidal conditions. Panel A represents spring high tide, while Panel B shows spring low tide. Current vectors are classified into five velocity ranges, revealing pronounced temporal and spatial variability.

During spring high tide (Figure 6A), current velocities are generally moderate to high, with widespread areas exhibiting speeds between 0.084-0.207~m/s, and localized zones exceeding 0.208~m/s, particularly north of Bedono and along the main tidal channels offshore from Sayung.

Currents are oriented predominantly eastward and northeastward, reflecting the flood tide inflow propagating across the shallow coastal plain. Higher velocities are evident adjacent to constricted flow pathways near the sea toll road alignment, where bathymetric steering accelerates tidal currents. In contrast, during spring low tide (Figure 6B), currents intensify substantially across much of the domain. Maximum velocities exceed 0.665 m/s, with the highest speeds concentrated in tidal channels and seaward of Bedono. Flow vectors display strong seaward orientation, indicating ebb-dominated transport as tidal water drains rapidly from intertidal flats and estuarine channels. The spatial extent of high-velocity zones is more pronounced during low tide, reflecting enhanced tidal flushing and increased flow concentration through narrow inlets.

Figure 7 presents simulated surface current distributions during neap tidal conditions along the Semarang–Demak coastline. Panel A illustrates current patterns at neap high tides, whereas Panel B depicts conditions at neap low tides. Current velocities are categorized into five intervals, ranging from near-zero flows to maximum speeds exceeding 0.313 m/s. During the neap high tidal condition (Figure 7A), current velocities are

generally low to moderate across much of the nearshore area. Most vectors fall within the 0.017–0.112 m/s range, with the lowest speeds observed in sheltered embayments near Trimulyo, Sriwulan, and the landward side of the planned sea toll road alignment. Higher velocities are concentrated around tidal inlets and the seaward flanks of Bedono, where localized accelerations exceed 0.113 m/s. The currents predominantly show eastward to northeastward flow directions, reflecting flood tide inflow and partial inundation of intertidal zones.

In contrast, neap low tide conditions (Figure 7B) are characterized by slightly stronger and more spatially extensive currents. While much of the domain still exhibits moderate velocities in the 0.026–0.099 m/s range, peak speeds exceed 0.313 m/s in several tidal channels and near the offshore margins. Flow directions shift predominantly towards the seaward, especially north of Bedono and along the main estuarine outflows near Sayung, indicating ebb tide drainage of intertidal flats.

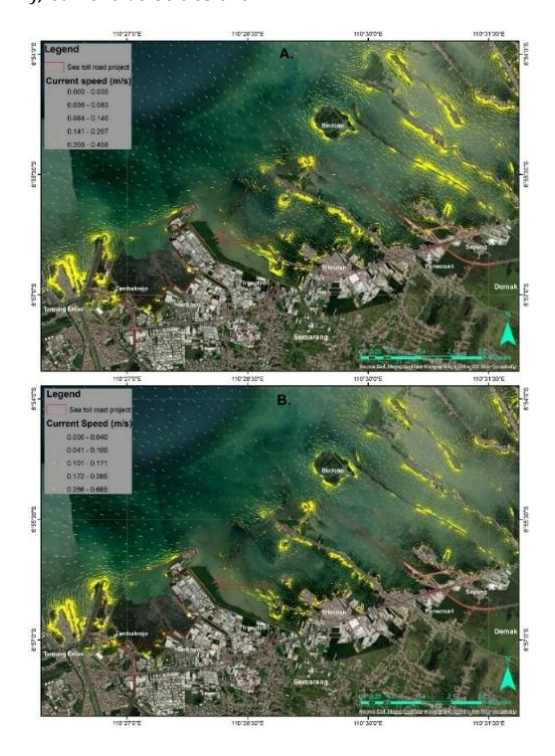


Figure 6: Tidal current patterns during spring tidal conditions; flood tides (A) and ebb tides (B).

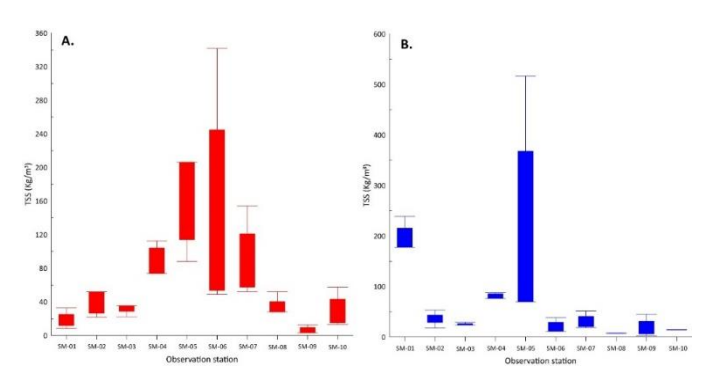


Figure 7: Tidal current patterns during neap tidal conditions; flood tides (A) and ebb tides (B)

#### 3.4 Sediment transport and morphological changes

Figure 8 illustrates the spatial variability of total suspended sediment (TSS) concentrations across ten observation stations (SM-01 to SM-10) during contrasting tidal phases. Panel A depicts TSS distributions measured during spring tides, while Panel B presents data from neap tides. During spring tides (Figure 8A), TSS concentrations are highly variable among stations, ranging from less than 20 kg/m³ at SM-09 to over 240 kg/m³ at SM-06. The highest mean concentrations were recorded at SM-06 (approximately 240 kg/m³, with variability extending beyond 320 kg/m³), followed by SM-05 and SM-04, which also exhibited elevated TSS levels exceeding 150 kg/m³. In contrast, stations SM-01, SM-02, SM-03, SM-08, and SM-09 consistently exhibited lower TSS values, generally below 50 kg/m³.

Neap tide conditions (Figure 8B) exhibited markedly lower TSS concentrations across most stations. The highest TSS was recorded at SM-05, with a mean exceeding 300 kg/m³, while the remaining stations predominantly ranged between 20 and 100 kg/m³. Notably, SM-01 maintained relatively high TSS even during neap tides, suggesting localized sediment resuspension or fluvial input. Overall, variability was reduced compared to spring tides, with fewer stations showing extreme TSS excursions.



**Figure 8:** Model-based TSS variability during the spring tidal condition (A) and the neap tidal condition (B)

Figure 9 shows the spatial distribution of bed level change across the Semarang–Demak nearshore zone, derived from hydrodynamic and sediment transport simulations. The changes range from +0.4 m (accretion) to -0.45 m (erosion), highlighting marked spatial heterogeneity. Substantial erosion zones (red and orange) are concentrated around Tanjung Emas and the Semarang port area, where bed lowering exceeds -0.35 m, as well as northeast of Bedono village, where similar magnitudes of scouring are evident. Moderate erosion also extends along the nearshore zone adjacent to Sayung and Purwosari. In contrast, significant sediment accretion (green areas) is observed offshore of Trimulyo, Sriwulan, and parts of the Demak coastline, with deposition thickness exceeding +0.3 m. Transitional zones with minor changes (-0.07 to +0.11 m) are distributed across intertidal flats and channels connecting Semarang and Demak.

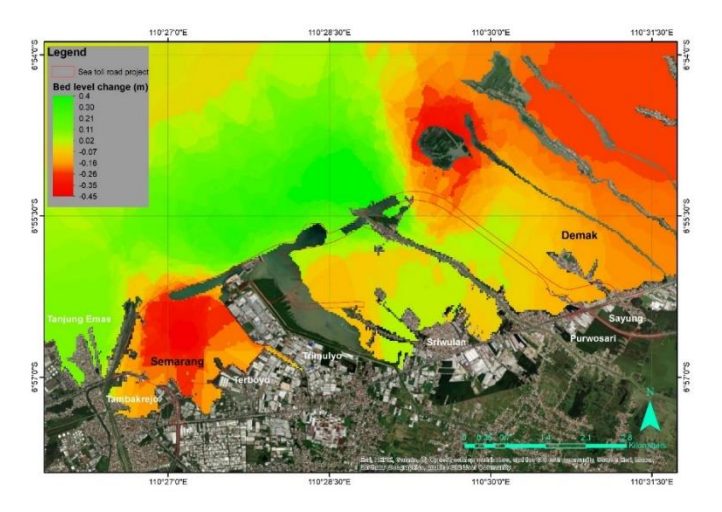


# Figure 9: Estimated bed level change during 30 days of simulation 4. DISCUSSION

The region of Sayung Subdistrict, up to the North Semarang region, is composed of alluvial rock formations, which include quarter tufa clay, clayey humus, sand, silt, and clay deposits (Thaden et al., 1975). The characteristics of silt and clay sediments indicate a weak current and wave energy in the surrounding waters. Cohesive silt tends to resist redistribution by water currents (Rahmadi et al., 2021). Based on the interpolated sediment texture map, areas near the sea embankment or toll road project are characterized by mixed-texture sediments, consisting of both fine and coarse particles (sand). The observation sites, which are located closer to the shoreline, river mouths, and mangrove areas, are expected to yield finer sediment sizes. However, the analysis shows the presence of coarser grains closer to land (the coast). This finding is consistent with several previous studies, indicating that fine-scaled sediment types, including silt, clay, and fine sand characterize the Demak coastal zones (Gemilang et al., 2021; Sihombing et al., 2021; Utomo et al., 2022).

Sediment grain size is typically strongly influenced by oceanographic processes in the vicinity of the sampling area. The movement of sea currents and river discharge has a significant impact on the characteristics of seabed sediment deposits. The sediment transported by either seawater or river water depends greatly on the flow velocity; the higher the flow velocity, the larger and more numerous the particles that can be carried (Nabila et al., 2021). The sediment texture characteristics in the study area suggest that river flow and discharge exert a stronger influence than ocean currents (during low tide), causing fine particles, such as silt, to settle farther away from the coast.

The sediment transport pattern consists of bedload transport and suspension transport. The bedload transport mechanism occurs with coarse sediment fractions carried by traction currents through rolling, dragging, and creeping processes (Dyer, 1986; Islam and Crawford, 2022). In contrast, suspended load transports finer fractions (ranging from clay to very fine sand) in suspension, allowing them to be carried over relatively long distances before settling when the current velocity decreases. This mechanism suggests that current characteristics near the shoreline are dominated by traction flow, resulting in the deposition of mixed coarse and fine sediment fractions. Meanwhile, as the current weakens toward the open sea, it predominantly deposits fine sediments such as silt.

Hydrodynamic analyses confirm that the area experiences a mixed, predominantly diurnal tidal regime, as evidenced by the dominance of the O1 and K1 constituents over the semidiurnal M2 and S2 components. The presence of shallow water overtides further highlights the nonlinear tidal distortion caused by bathymetric complexity and frictional damping. This tidal behavior produces temporally variable current intensities, which in turn influence both the timing and magnitude of sediment transport (Haigh et al., 2019).

Current rose diagrams illustrate spatial heterogeneity in tidal currents between monitoring stations. For instance, CM-01 exhibits bidirectional currents during neap tides and weaker, more unidirectional flows during spring tides, likely due to localized frictional effects. In contrast, CM-02 exhibits stronger and more consistent currents during spring tides, indicating more energetic conditions and a higher potential for sediment transport. These variations underscore the importance of spatially explicit calibration for hydrodynamic and sediment transport models.

Model validation demonstrates a strong agreement between observed and simulated tidal elevations, with residual errors generally within ±0.05 m. This level of accuracy confirms the reliability of the hydrodynamic simulations for further scenario analysis (Wisha et al., 2022). The contrasting current patterns during spring high and low tides highlight the asymmetric forcing that drives sediment dynamics: moderate inflows during high tides facilitate deposition in sheltered areas. In contrast, energetic ebb flows during low tides enhance sediment resuspension and export, particularly around Bedono and Sayung.

Crucially, simulation results underline the profound impact of the Semarang–Demak sea toll road development. The alignment intersects dynamic sediment redistribution zones, characterized by alternating periods of erosion and deposition. Spring ebb tides generate currents exceeding 0.6 m/s, intensifying scouring potential along embankment foundations. Conversely, neap tide conditions promote localized fine

sediment deposition around embankment toes, heightening the risk of differential settlement and shoaling. Comparable challenges have been documented in the construction of linear coastal infrastructure, including Japan's Isahaya Bay polder and China's coastal reclamation projects, where altered hydrodynamics accelerated erosion and sediment trapping in adjacent zones(Wang et al., 2014; Jia et al., 2018).

TSS measurements further reinforce this pattern. Spring tides produce substantially elevated suspended sediment concentrations, especially at mid-reach stations such as SM-05 and SM-06, reflecting intensified resuspension under stronger currents. Conversely, neap tides generally exhibit lower TSS levels, with localized hotspots often linked to fluvial input or human disturbance. This variability highlights the importance of incorporating spring-neap cycles into sediment management planning. Bed level change simulations reveal areas of pronounced erosion near Tanjung Emas Port and northeast of Bedono, consistent with zones of high current velocity and sediment export. In contrast, deposition zones offshore from Sriwulan and Demak indicate sediment sinks where fine particles accumulate under calmer hydrodynamic conditions. Critically, the sea toll road corridor traverses areas with contrasting erosion and accretion patterns, raising concerns over differential seabed response and potential impacts on structural stability.

Overall, the combined evidence suggests that without adaptive design measures, such as scour protection, sediment bypassing structures, or engineered sediment buffers, the toll road project is likely to exacerbate erosion risk, compromise foundation stability, and disrupt sediment continuity. The study highlights the importance of adopting integrated sediment management frameworks, continuous monitoring, and flexible engineering solutions, in line with global best practices for sustaining infrastructure resilience and coastal ecosystem health in dynamic estuarine environments.

#### 5. CONCLUSION

This study demonstrates that sediment dynamics and morphological evolution along the Semarang coast — the interplay of a mixed diurnal tidal regime, river discharge, and human activities - strongly govern the Demak coast. The contrasting distribution of fine sediments offshore and coarser deposits near the shoreline reflects spatial variability in current energy and sediment transport pathways. Hydrodynamic modeling and TSS observations confirm that spring tides markedly intensify resuspension and sediment export, while neap tides promote deposition and relative seabed stability. Critically, the alignment of the sea toll road project traverses zones with active sediment redistribution and variable bed level changes. This finding raises concerns about localized scour, differential settlement, and altered flow patterns that could compromise embankment stability and exacerbate coastal erosion. These findings underscore the need for adaptive engineering solutions, continuous sediment monitoring, and integrated coastal management strategies to mitigate infrastructure risks and sustain estuarine resilience in this dynamic environment.

# ACKNOWLEDGMENT

We would like to express our sincere gratitude to the Department of Aquatic Resource Management, Diponegoro University, for their continuous support throughout the course of this study. We also extend our appreciation to the local government authorities and community members for their invaluable assistance and cooperation during the field survey.

#### REFERENCES

- Andreas, H., Abidin, H. Z., Sarsito, D. A., and Pradipta, D. 2018. Insight analysis on dyke protection against land subsidence and the sea level rise around northern coast of Java (PANTURA) Indonesia. Geoplanning: Journal of Geomatics and Planning, 5(1), Pp. 101-114. https://doi.org/10.14710/geoplanning.5.1.101-114
- Astuti, S., Muryani, C., and Rindarjono, M. G. 2018. The community participation on mangrove conservation in Sayung, Demak from 2004-2016. In IOP Conference Series: Earth and Environmental Science (Vol. 145, No. 1, p. 012087). IOP Publishing. https://doi.org/10.1088/1755-1315/145/1/012087
- Baskoro, H., Atmodjo, W., and Purwanto, P. 2016. Studi Pengaruh Gelombang Terhadap Kerusakan Bangunan Pantai Hybrid Engineering Di Desa Timbulsloko, Demak. Journal of Oceanography, 5(3), Pp. 340-348.

- Chrysanti, A., Adhani, A., Azkiarizqi, I. N., Adityawan, M. B., Kusuma, M. S. B., and Cahyono, M. 2024. Assessing Compound Coastal–Fluvial Flood Impacts and Resilience Under Extreme Scenarios in Demak, Indonesia. Sustainability, 16(23), 10315. https://doi.org/10.3390/su162310315
- Dewi, R. S., and Bijker, W. 2020. Dynamics of shoreline changes in the coastal region of Sayung, Indonesia. The Egyptian Journal of Remote Sensing and Space Science, 23(2), Pp. 181-193. https://doi.org/10.1016/j.ejrs.2019.09.001
- Dyer, K. R. 1986. Coastal and estuarine sediment dynamics. Chichester: John Wiley and Sons.
- Folk, R. L., and Ward, W. C. 1957. Brazos River bar: a study in the significance of grain size parameters. Journal of Sedimentary Research, 27(1), Pp. 3–26. https://doi.org/10.1306/74D70646-2B21-11D7-8648000102C1865D
- Gemilang, W. A., Wisha, U. J., Solihuddin, T., Arman, A., and Ondara, K. 2020. Sediment accumulation rate in sayung coast, Demak, central java using unsupported 210 Pb isotope. Atom Indonesia, 46(1), Pp. 25-32. https://doi.org/10.17146/aij.2020.935
- Hafid, H., Thaha, M. A., Maricar, F., and Bakri, B. 2021. Hybrid engineering on permeable groins to reduce the longshore current. In IOP Conference Series: Earth and Environmental Science (Vol. 841, No. 1, p. 012025). IOP Publishing. https://doi.org/10.1088/1755-1315/841/1/012025
- Haigh, I. D., Pickering, M. D., Green, J. M., Arbic, B. K., Arns, A., Dangendorf, S., Hill, D. F., Horsburgh, K., Howard, T., Idier, D., Jay, D. A., Janicke, L., Lee, S. B., Muller, M., Schidelegeger, M., Talke, S. A., Wilmes, S., and Woodworth, P. L. 2020. The tides they are a-Changin': A comprehensive review of past and future nonastronomical changes in tides, their driving mechanisms, and future implications. Reviews of Geophysics, 58(1), e2018RG000636. https://doi.org/10.1029/2018RG000636
- Hamidifar, H., Nones, M., and Rowinski, P. M. 2024. Flood modeling and fluvial dynamics: A scoping review on the role of sediment transport. Earth-Science Reviews, 253, 104775. https://doi.org/10.1016/j.earscirev.2024.104775
- Hsieh, H. L. 1995. Spatial and temporal patterns of polychaete communities in a subtropical mangrove swamp: influences of sediment and microhabitat. Marine Ecology Progress Series, 127, Pp. 157–167. https://doi.org/10.3354/meps127157
- Hubbard, J. A. E. B., and Pocock, Y. P. 1972. Sediment rejection by recent scleractinian corals: a key to palaeo-environmental reconstruction. Geologische Rundschau, 61(2), Pp. 598–626.
- Islam, M. S., and Crawford, T. W. 2022. Assessment of Spatio-Temporal Empirical Forecasting Performance of Future Shoreline Positions. Remote Sensing, 14(24). https://doi.org/10.3390/rs14246364
- Ismanto, A., Zainuri, M., Hutabarat, S., Sugianto, D. N., Widada, S., and Wirasatriya, A. 2017. Sediment transport model in sayung district, demak. In IOP Conference Series: Earth and Environmental Science (Vol. 55, No. 1, p. 012007). IOP Publishing. https://doi.org/10.1088/1755-1315/55/1/012007
- Jafarzadegan, K., Moradkhani, H., Pappenberger, F., Moftakhari, H., Bates, P., Abbaszadeh, P., Marsooli, R., Ferreira, C., Cloke, H. L., Ogden, F., and Duan, Q. 2023. Recent advances and new frontiers in riverine and coastal flood modeling. Reviews of Geophysics, 61(2), e2022RG000788. https://doi.org/10.1029/2022RG000788
- Jamaludin, H., and Mahdi, Z. 2025. Community Resistance to Development of The Semarang-Demak Sea Embankment Toll Road. The Journal of Academic Science, 2(4), Pp. 1046-1065. https://doi.org/10.59613/3gqcpc82
- Jia, R., Lei, H., Hino, T., and Arulrajah, A. 2018. Environmental changes in Ariake Sea of Japan and their relationships with Isahaya Bay reclamation. Marine pollution bulletin, 135, Pp. 832-844. https://doi.org/10.1016/j.marpolbul.2018.08.008
- Marfai, M. A., Tyas, D. W., Nugraha, I., Fitriatul'Ulya, A., and Riasasi, W. 2016. The morphodynamics of Wulan Delta and its impacts on the coastal community in Wedung subdistrict, Demak regency, Indonesia. Journal of Environmental Protection, 7(1), Pp. 60-71. https://doi.org/10.4236/jep.2016.71006
- Nabila, A., Marwoto, J., Subardjo, P., Rifai, A., and Atmodjo, W. 2021. Analisa Laju Sedimentasi di Dermaga 4 Pelabuhan Cigading 1 Provinsi Banten.

- Indonesian Journal of Oceanography, 3(1), Pp. 36–43. https://doi.org/10.14710/ijoce.v3i1.9901
- Pamungkas, G. B. 2021. The Land Acquisition of Inundated Land for The Toll Road Project of Semarang-Demak Sea Embankment. The Indonesian Journal of Planning and Development, 6(2), Pp. 48-55. https://doi.org/10.14710/ijpd.6.2.48-55
- Pamungkas, G. B. 2021. The Land Acquisition of Inundated Land for The Toll Road Project of Semarang-Demak Sea Embankment. The Indonesian Journal of Planning and Development, 6(2), Pp. 48-55.
- Rahmadi, N., Widada, S., Marwoto, J., Atmodjo, W., and Widiaratih, R. 2021. Studi Sebaran Sedimen Dasar di Perairan Sungai Banjir Kanal Timur Semarang, Jawa Tengah. Indonesian Journal of Oceanography, 3(3), Pp. 286–294. https://doi.org/10.14710/ijoce.v3i3.11707
- Rimba, A. B., Osawa, T., Parwata, I. N. S., As-syakur, A. R., Kasim, F., and Astarini, I. A. 2018. Physical assessment of coastal vulnerability under enhanced land subsidence in Semarang, Indonesia, using multi-sensor satellite data. Advances in Space Research, 61(8), Pp. 2159-2179. https://doi.org/10.1016/j.asr.2018.01.026
- Sarah, D., Hutasoit, L. M., Delinom, R. M., and Sadisun, I. A. 2020. Natural compaction of Semarang-Demak alluvial plain and its relationship to the present land subsidence. Indonesian Journal on Geoscience, 7(3), Pp. 273-289. https://doi.org/10.17014/ijog.7.3.273-289
- Satyana, A. H. 2006. New Insight on Tectonics of Central Java, Indonesia and Its Petroleum Implications. In American Association of Petroleum Geologists (AAPG) International Conference and Exhibition (p. 90061).
- Sihombing, D. Y. S., Zainuri, M., Maslukah, L., Widada, S., and Atmodjo, W. 2021. Studi Sebaran Ukuran Butir Sedimen Di Muara Sungai Jajar, Demak, Jawa Tengah. Indonesian Journal of Oceanography, 3(1), Pp. 111–119. https://doi.org/10.14710/ijoce.v3i1.10665
- Solahudin, D. S., Satria, B. A., and Jannah, N. T. 2024. Analisa DPSIR Pembangunan Tol Semarang-Demak dan Kawasan Ekosistem Mangrove di Wilayah Pesisir Semarang-Demak. Journal of Syntax Literate, 9(8).
- Solihuddin, T., Husrin, S., Salim, H. L., Kepel, T. L., Mustikasari, E., Heriati, A., Ati, R. N. A., Purbani, D., Indiasari, V. Y., and Berliana, B. 2021. Coastal erosion on the north coast of Java: adaptation strategies and coastal management. In IOP Conference Series: Earth and Environmental Science (Vol. 777, No. 1, p. 012035). IOP Publishing. https://doi.org/10.1088/1755-1315/777/1/012035
- Solihuddin, T., Triana, K., Rachmayani, R., Husrin, S., Pramudya, F. A., Salim,

- H. L., Heriati, A., and Suryono, D. 2024. The impact of coastal erosion on land cover changes in Muaragembong, Bekasi, Indonesia: a spatial approach to support coastal conservation. Journal of Coastal Conservation, 28, 43. https://doi.org/10.1007/s11852-024-01045-2
- Sugianto, D. N., Widiaratih, R., Widada, S., Suripin, , Handayani, E. P., and Cahyaningtyas, P. 2022. Analysis of structural and non-structural disaster mitigation due to erosion in the Timbulsloko Village, Demak-Central Java. Journal of Ecological Engineering, 23(2), Pp. 246-254. https://doi.org/10.12911/22998993/144559
- Thaden, R. E., Sumadirdja, H., and Richards, P. W. 1975. Peta Geologi Lembar Magelang dan Semarang, Jawa. Bandung.
- Utomo, G. J., Atmodjo, W., Sugianto, D. N., Widiaratih, R., and Ismanto, A. 2022. Efektifitas Struktur Kerapatan terhadap Laju Sedimentasi dan Jenis Sedimen pada Hybrid Engineering di Desa Timbulsloko, Demak, Jawa Tengah. Indonesian Journal of Oceanography, 4(1), Pp. 47–58. https://doi.org/10.14710/ijoce.v4i1.13160
- Van Wesenbeeck, B. K., Balke, T., van Eijk, P., Tonneijck, F., Siry, H. Y., Rudianto, M. E., and Winterwerp, J. C. 2015. Aquaculture induced erosion of tropical coastlines throws coastal communities back into poverty. Ocean and Coastal Management, 116, 466-469. https://doi.org/10.1016/j.ocecoaman.2015.09.004
- Wang, W., Liu, H., Li, Y., and Su, J. 2014. Development and management of land reclamation in China. Ocean and Coastal Management, 102, Pp. 415-425. https://doi.org/10.1016/j.ocecoaman.2014.03.009
- Wentworth, C. K. 1922. A scale of grade and class terms for clastic sediments. Journal of Geology, 30(5), Pp. 377–392.
- Wisha, U. J., Gemilang, W. A., Wijaya, Y. J., and Purwanto, A. D. 2022. Model-based estimation of plastic debris accumulation in Banten Bay, Indonesia, using particle tracking-Flow model hydrodynamics approach. Ocean and Coastal Management, 217, 106009. https://doi.org/10.1016/j.ocecoaman.2021.106009
- Yasin, A. M., Sukiyah, E., and Isnaniawardhani, V. 2016. Grain Size Analysis of Quartenary Sediment from Kendari Basin, Indonesia. International Journal of Science and Research (IJSR), 5(11), Pp. 1748–1751. https://doi.org/10.21275/ART20163165
- Yuan, S., Tang, H., Li, K., Xu, L., Xiao, Y., Gualtieri, C., Rennie, C., and Melville, B. 2021. Hydrodynamics, sediment transport and morphological features at the confluence between the Yangtze River and the Poyang Lake. Water Resources Research, 57(3), e2020WR028284. https://doi.org/10.1029/2020WR028284

